Enzyme-assisted self-assembly under thermodynamic control

ARTICLE *in* NATURE NANOTECHNOLOGY · FEBRUARY 2009

Impact Factor: 34.05 · DOI: 10.1038/nnano.2008.378 · Source: PubMed

6 AUTHORS, INCLUDING:

Richard J. Williams
RMIT University
24 PUBLICATIONS **871** CITATIONS
SEE PROFILE

Andrew Smith
The University of Manchester
30 PUBLICATIONS **2,226** CITATIONS
SEE PROFILE

Richard F Collins
The University of Manchester
51 PUBLICATIONS **2,268** CITATIONS
SEE PROFILE

nature nanotechnology

LETTERS

PUBLISHED ONLINE: 21 DECEMBER 2008 | DOI: 10.1038/NNANO.2008.378

Enzyme-assisted self-assembly under thermodynamic control

Richard J. Williams[1,2], Andrew M. Smith[1,2], Richard Collins[2], Nigel Hodson[3], Apurba K. Das[1,2†] and Rein V. Ulijn[1,2†*]

The production of functional molecular architectures through self-assembly is commonplace in biology, but despite advances[1–3], it is still a major challenge to achieve similar complexity in the laboratory. Self-assembled structures that are reproducible and virtually defect free are of interest for applications in three-dimensional cell culture[4,5], templating[6], biosensing[7] and supramolecular electronics[8]. Here, we report the use of reversible enzyme-catalysed reactions to drive self-assembly. In this approach, the self-assembly of aromatic short peptide derivatives[9,10] provides a driving force that enables a protease enzyme to produce building blocks in a reversible and spatially confined manner. We demonstrate that this system combines three features: (i) self-correction—fully reversible self-assembly under thermodynamic control; (ii) component-selection—the ability to amplify the most stable molecular self-assembly structures in dynamic combinatorial libraries[11–13]; and (iii) spatiotemporal confinement of nucleation and structure growth. Enzyme-assisted self-assembly therefore provides control in bottom-up fabrication of nanomaterials that could ultimately lead to functional nanostructures with enhanced complexities and fewer defects.

Laboratory-based self-assembly processes are driven by (gradual) changes in conditions, such as solvent polarity, ionic strength, temperature, pH or concentration of inorganic/organic molecules. In contrast, in biological systems, self-assembly usually occurs under conditions that are constant overall, and is tightly regulated by spatially confined molecular mechanisms. Researchers are increasingly seeking to mimic biology's approaches in an effort to enhance control over bottom-up nanofabrication processes. One emerging concept consists of making use of the catalytic action of enzymes to control self-assembly. In this approach, enzymes convert non-assembling precursors into self-assembling components (or vice versa), for example, by hydrolysis or ATP-driven formation of (phosphate) esters[9,14,15], transacylation[16,17] or DNA ligation[18]. In these systems, production of self-assembly components is (indirectly) driven by hydrolytic reactions that are thermodynamically downhill. As a result, the production of building blocks and self-assembly are both favoured in isolation and thermodynamically uncoupled. We hypothesize that direct coupling of enzyme action with self-assembly may be achieved by making use of enzymatic reactions that are in themselves thermodynamically unfavoured, yet involve relatively small free energy changes. Amide hydrolysis reactions are close to equilibrium[19] under dilute aqueous conditions (for a typical peptide $\Delta G^0_{\text{amide hydrolysis}} = -4.0\,\text{kJ mole}^{-1}$ at pH 7.5, 25 °C) (see Supplementary Information) and can be shifted towards amide formation by relative stabilization of the amide component, for example, through formation of a self-assembled structure (when $\Delta G_{\text{self-assembly}} - \Delta G_{\text{amide hydrolysis}} < 0$) (Fig. 1b). Indeed, we have previously demonstrated protease-driven molecular self-assembly by direct condensation of non-assembling precursors to self-assembling peptide derivatives[20].

A reversible system of this type will operate under thermodynamic control, and will ultimately favour formation of the most stable structures, the reversibility of the system assuring that (kinetically trapped) imperfections are corrected. It opens up opportunities for dynamic combinatorial libraries (DCL)[11–13], an approach that has been used extensively to identify molecular interactions and folding events[21] through thermodynamically driven component selection. Although peptide libraries have been exploited before in dynamic combinatorial experiments involving disulphide exchange[22,23] or metal binding[24], a dynamic library system that reversibly exchanges peptide bonds[25] allows access to peptide sequence libraries. With one exception[13] the use of DCL for the discovery of stable supramolecular materials is an unexplored area[11].

A final characteristic of enzyme-assisted self-assembly relates to the possibility of spatially confining structure growth at the initial stages of the self-assembly process. Because building blocks are necessarily produced at the site of enzyme action, that is, in close proximity and in a confined nanoscopic space, enzyme-assisted self-assembly may therefore favour structure formation at the site of enzyme action.

In this Letter, we explore these three features, namely (i) fully reversible self-assembly, (ii) component selection and (iii) spatiotemporal confinement of structure growth, thereby significantly enhancing control over molecular self-assembly.

The self-assembly precursors consisted of *N*-(fluorenyl-9-methoxycarbonyl)-protected amino acids (glycine, G; leucine, L; phenylalanine, F; threonine, T) with a fourfold excess of nucleophile (G_2, F_2, L_2 dipeptides or L-, F-OMe amino-acid esters) (Fig. 1a). A non-specific endoprotease (thermolysin) was used to catalyse peptide bond formation and hydrolysis. Fmoc-peptides that are formed then self-assemble through the formation of antiparallel β-sheets with fluorenyl groups presented at alternating sides interlocking multiple sheets through π-stacking (Fig. 1b). The resulting arrays of sheets may, in turn, form cylindrical structures when both edges of an array of β-sheets lock together[10]. Figure 2 summarizes the results obtained for Fmoc-F and F_2. This system initially appears as a milky suspension and over 60 min forms a transparent self-supporting hydrogel (Fig. 2a), which correlates with nanostructure formation, as visualized using transmission electron microscopy (TEM). Nanoscale fibres propagate over time, increasing both in length and density until an entangled network is formed (Fig. 2b). Time-dependent formation of Fmoc-peptides could be analysed by high-pressure liquid chromatography (HPLC). Over the first 3 h,

[1]School of Materials, The University of Manchester, Oxford Road, Manchester M13 9PL, UK, [2]Manchester Interdisciplinary Biocentre, The University of Manchester, Oxford Road, Manchester M13 9PL, UK, [3]Faculty of Life Sciences, The University of Manchester, Manchester M13 9PT, UK; †Present address: Department of Pure and Applied Chemistry/WestCHEM, The University of Strathclyde, Glasgow G1 1XL, UK; *e-mail: Rein.Ulijn@strath.ac.uk

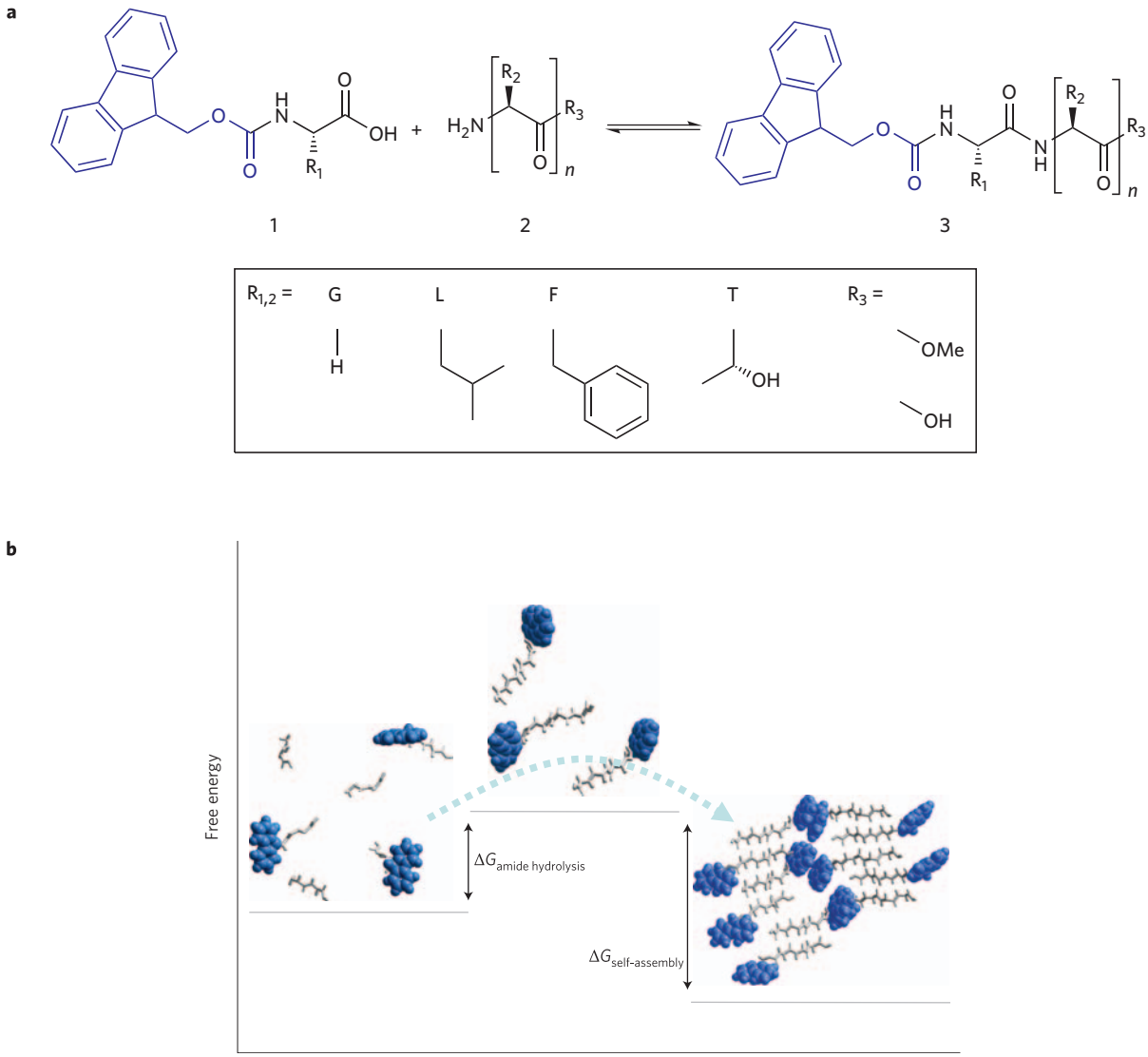

Figure 1 | Enzyme-assisted self-assembly under thermodynamic control. a, Reversed hydrolysis reaction in which peptide derivatives **3** are formed from a Fmoc-amino acid **1** and a dipeptide or amino acid ester **2. b**, Diagram showing the free energy profile of enzyme-assisted self-assembly of peptide derivatives. Peptide derivatives are shown schematically in grey (amino acids) and blue (Fmoc). Amide formation is thermodynamically unfavoured ($\Delta G_{\text{amide hydrolysis}}$) and will only occur when building blocks are produced that form thermodynamically stable structures (determined by $\Delta G_{\text{self-assembly}}$). Also shown is a molecular model of the resulting structures, with the stacked Fmoc group (blue) and peptide side chains (grey) arranged into an antiparallel beta sheet structure; the example here is of an Fmoc-tripeptide (the side chains are not shown).

a distribution of Fmoc-peptides had formed, with Fmoc-F_3 predominating and the relative distribution of components remaining unchanged over 300 h (Fig. 2c). Structural changes, as measured by fluorescence spectroscopy and circular dichroism (CD), continued to occur significantly after a constant distribution had been achieved (Fig. 2d). Over time, the emission intensity of a broad peak centred at 440 nm gradually increased, indicative of a rearrangement of fluorenyl groups into extensive J-aggregates (Fig. 2d; see also Supplementary Information, Fig. S1c)[10]. Continuing enhancement of the CD signal at 307 nm during this time period shows an increase in chiral ordering of fluorenyl groups (Fig. 2d; see also Supplementary Information, Fig. S1c). Similar results were obtained for Fmoc-L/L_2 (see Supplementary Information, Fig. S1a,b,d). In order to test whether these systems evolve towards an equilibrium state, that is, are under thermodynamic control, a competition experiment was designed involving Fmoc-T with two nucleophiles, L-OMe and F-OMe, as precursors. Although both peptide derivatives were formed in high yield in isolation (84 and 96%), it was found that in direct competition the Fmoc-TL-OMe peptide was produced at ~14% and the F peptide at ~82%, suggesting that the latter peptide derivatives self-assemble more favourably (Fig. 3a). In a sequential experiment, where Fmoc-T/L-OMe that had reached a constant conversion (~84%) was exposed to the competing nucleophile, F-OMe, a rearrangement of the predominantly Fmoc-TL-OMe to Fmoc-TF-OMe was observed, which ultimately gave rise to the same distribution as observed for the competition experiment (Fig. 3a). These results demonstrate that enzyme-assisted self-assembly systems are fully reversible and equilibrium driven. Clearly, the most stable components are favoured, with the component distribution determined by the free energy landscape (Fig. 3a, inset).

The DCL concept was further demonstrated using the Fmoc-L/L_2 system (Fig. 3b), which, in the presence of a non-specific protease gives rise to an Fmoc-L_n oligomer distribution as a result of continued (reversed) hydrolysis over time. During the initial stage (up to 100 h), the major peptide derivative that formed was Fmoc-L_3 (with over 50% Fmoc-L still present). Over the course of 3,000 h, the system was remodelled, eventually reaching a constant distribution where the major peptide component was Fmoc-L_5

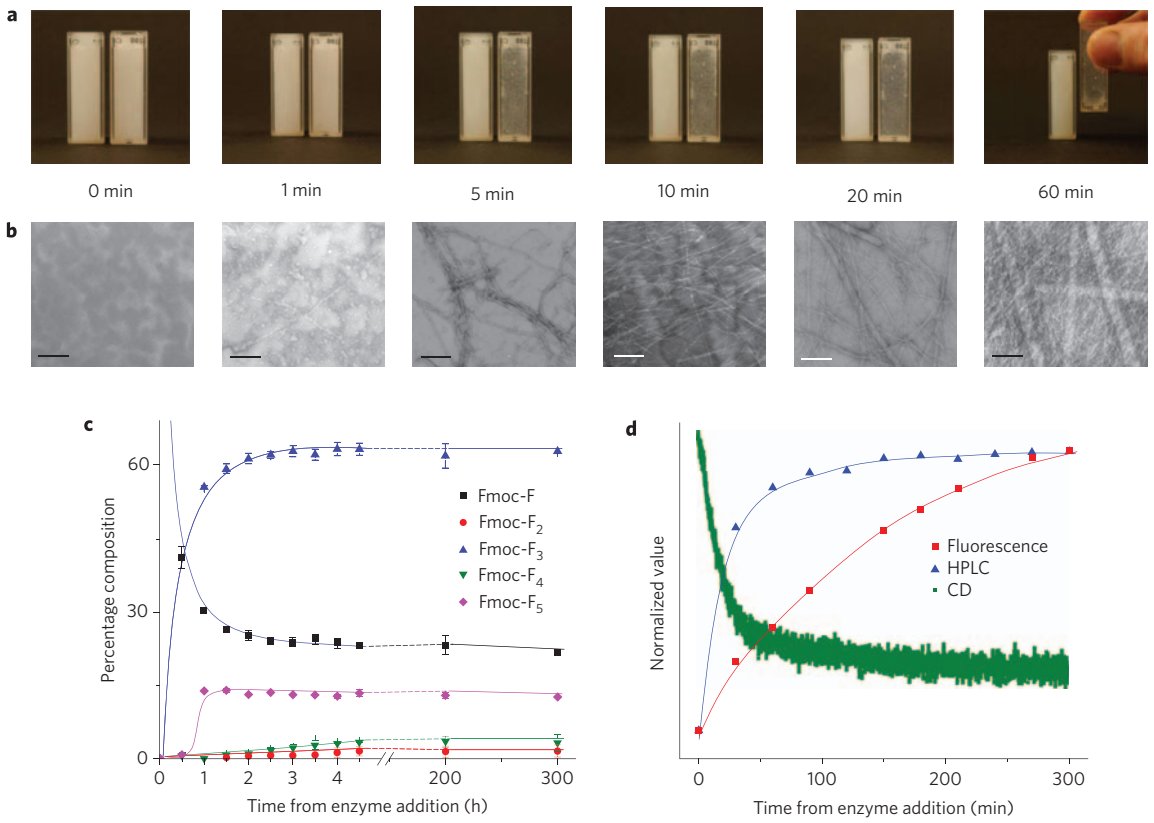

Figure 2 | Enzyme-assisted self-assembly of Fmoc-peptide derivatives. a, Milky suspension containing Fmoc-F and F_2 in the presence of 0.5 mg ml^{-1} thermolysin undergoing a visible change to a transparent self-supporting gel. **b**, Corresponding TEM micrographs demonstrating the formation of an entangled network of nanoscopic fibres (scale bars, 100 nm). **c**, HPLC time course for the distribution of Fmoc-F_n derivatives at various times after the addition of enzyme. **d**, Comparison of the percentage conversion to the self-assembling Fmoc-F_3, as measured by HPLC (only Fmoc-F_3 is shown for clarity), with structural changes observed by fluorescence spectroscopy and circular dichroism (CD), which demonstrates the structural correction of the Fmoc-F_n system.

(~71%). Similar distributions, with Fmoc-L_5 predominating, were observed when different starting points were used (see Supplementary Information, Table S1). TEM (see Supplementary Information, Fig. S2) and atomic force microscopy (AFM) analysis (Fig. 3c) revealed that the conversion of predominantly Fmoc-L_3 to Fmoc-L_5 corresponds to major morphological changes, from fibres to sheet-like structures. These morphological changes coincide with significant spectroscopic changes. Fluorescence spectroscopy showed, before enzyme addition, an emission maximum centred on 320 nm with a shoulder at 350 nm representing the fluorenyl excimer[26,27] (Fig. 3d). Rearrangement of molecules into an extensive J-aggregate of fluorenyl rings, centred at 440 nm, stabilized by π-stacking interactions, was observed at 5 h (Fig. 3d). When Fmoc-L_5 predominates (from 500 h) a change in fluorescence emission is observed, with an intense excimer peak dominating the spectrum, suggesting that the sheet-like assemblies that are observed for Fmoc-L_5 have a notably different fluorenyl conformation. Fourier transform infrared spectroscopy (FTIR) analysis at 0, 5 and 3,000 h consistently shows well-defined bands centred around 1,630 cm^{-1} and 1,680–1,690 cm^{-1}, consistent with the formation of antiparallel β-sheet structures[28] (Fig. 3d). These results demonstrate that antiparallel β-sheets dominate the peptide interactions in both Fmoc-L_3 and Fmoc-L_5 systems, and fluorenyl interactions change with peptide length. Remodelling from fibres to sheets may be related to the energetic penalty of solvent-exposed fluorenyl groups that is outweighed by a more favourable arrangement of longer peptides in a β-sheet[10].

Finally, we demonstrate that enzyme-assisted self-assembly allows for localized structure nucleation and growth, a property that relates to the self-assembly kinetics of the system. At the early stages of the self-assembly process nucleation could be visualized both by TEM and AFM. Figure 4a shows example fields of TEM images of an Fmoc-L/L_2 system obtained 5 min after addition of enzyme. Fibres can be observed propagating from spherical structures of approximately 30 nm in diameter. As enzymatic formation of building blocks is localized, it appears likely that self-assembly nucleates close to enzyme molecules. This may suggest that each sphere contains (a small number of) enzyme molecule(s) (diameter < 2 nm) from which fibres propagate over time. To confirm whether self-assembly indeed occurs exclusively in the vicinity of enzymes, thermolysin was covalently attached to a di-amino polyethylene glycol (PEG) modified surface, with the surface left partially unmodified, creating a defined interface. Upon immersion of this modified surface into a solution containing precursors Fmoc-L and L_2, self-assembled structures were exclusively formed in the area containing the enzyme, observed using Congo Red, a birefringent dye for anisotropic structures (Fig. 4c,d) (see Supplementary Information, Fig. S3, for control experiments). These results show that enzyme assisted self-assembly favours spatial confinement of structure growth during the initial stages of the self-assembly process.

In summary, we have demonstrated the use of fully reversible enzyme reactions to direct self-assembling peptides through the free energy landscape. Three features of this system were explored. First, we demonstrated that this system is fully reversible and allows for structural correction. Second, we demonstrated that the system allows for the discovery of stable self-assembled nanostructures through component selection. Although enzymes have been used before to generate DCLs[29], the current approach opens up the possibility of making use of the versatility of peptides in the discovery of new soft materials. Finally, we show that structure

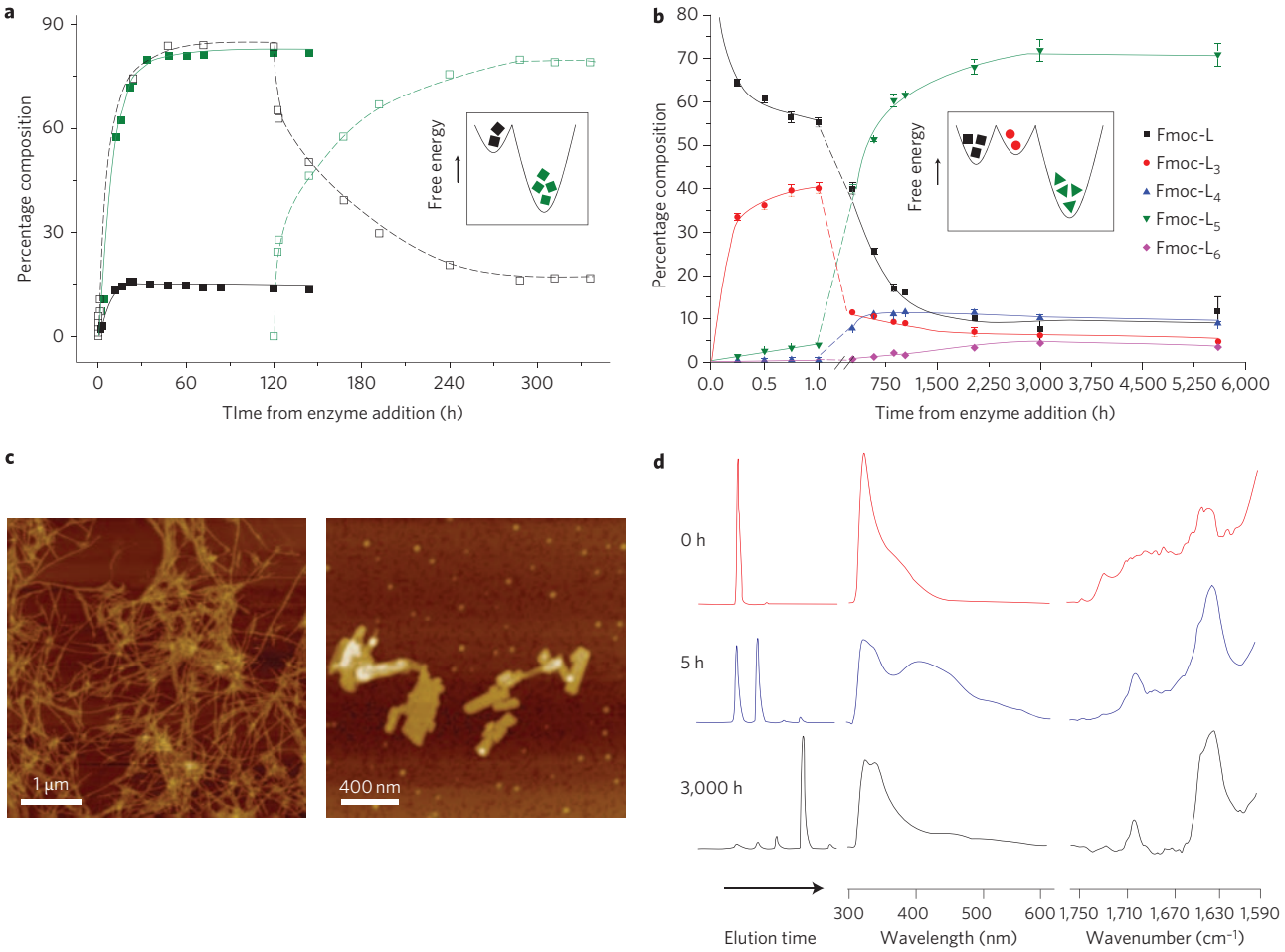

Figure 3 | Enzyme-driven dynamic combinatorial library. a, Enzyme-assisted self-assembly reactions performed using thermolysin and a mixture of Fmoc-T, F-OMe and L-OMe generates a distribution of the two possible peptide products: Fmoc-TF-OMe (green) and Fmoc-TL-OMe (black) (solid lines, closed symbols). A time course experiment performed with Fmoc-T and L-OMe using thermolysin (0.5 mg ml^{-1}) generates peptide Fmoc-TL-OMe. Subsequent addition of F-OMe, resulted in near complete replacement with Fmoc-TF-OMe, reaching an equilibrium distribution at 14 days, displaying a similar distribution to the direct competition experiment (dashed line, open symbol). The inset shows a schematic representation of the relative free energy differences between the peptide derivatives. **b**, HPLC time course for Fmoc-L_n with an enzyme concentration of 0.5 mg ml^{-1}. Up to 5 h, Fmoc-L_3 is predominantly formed (~47%). From 250 h, Fmoc-L_5 starts to dominate, continuing to dominate at the last time point at ~5,600 h (~70%), with Fmoc-L_4 and Fmoc-L_6 also formed. **c**, AFM imaging of the fibrillar structures formed at 5 min after enzyme addition (left) and the sheet-like structures observed after 2,000 h (right) show that the redistribution of derivatives is accompanied by a remodelling from fibres to sheet-like structures. **d**, Spectroscopic characterization immediately after enzyme addition, at 5 h, and at 3,000 h. HPLC chromatograms show the predominant formation of Fmoc-L_3 after 5 h and Fmoc-L_5 at 3,000 h. Fluorescence emission at 5 h shows the development of a broad feature in the region 400–500 nm, which appears upon formation of the gel, and which reduces in favour of a strong excimer signal at 3,000 h, suggesting significant molecular reorganization. FTIR analysis reveals consistent evidence of antiparallel β-sheets in the amide I region.

formation occurs in a spatiotemporally confined manner that may add an extra level of control to early stages of self-assembly. Indeed, nanoscale confinement is a key feature of the formation of complex dynamic structures in biological systems[30]. Overall, we believe that enzyme-assisted self-assembly provides an important step forward in directed self-assembly and in the discovery of peptide-based nanomaterials, paving the way to bottom-up fabrication of nanostructures with enhanced complexities and fewer defects.

Methods

All reagents were purchased from commercial sources at the highest purity and were used as supplied, unless stated otherwise in the experimental procedures.

Enzyme-assisted self-assembly. Fmoc-amino acids, dipeptides and amino acid esters were supplied by Bachem, Germany. Precursors were solubilized and homogeneously dispersed by the dropwise addition of 0.5 M NaOH, then gradually neutralized to pH 7 through sequential addition of 50 μl aliquots of 0.1 M HCl while vortexing. Fmoc-Thr-OH and amino acid methyl esters were solubilized in 0.1 M phosphate buffer at pH 8. Final mixtures contained 20 mmol l^{-1} Fmoc-amino acid and 80 mmol l^{-1} of the nucleophile in 800 μl obtained by the addition of purified H_2O. Thermolysin was supplied by Sigma Aldrich in the form of a lyophilized powder from *Bacillus thermoproteolyticus rokko* at 40 units mg^{-1}. This was reconstituted in H_2O to a volume of 200 μl and added to the precursor mixture to a final volume of 1,000 μl. Solutions were vortexed during the 20 s before sample extraction.

HPLC. A Dionex P680 HPLC system equipped with a Macherey-Nagel C18 column of 250 mm length, 4.6 mm internal diameter and 5 μm particle size was used to quantify conversions to peptide derivatives. The gradient used was a linear exchange between 40% acetonitrile in water at 2.5 min to 90% acetonitrile/water at 23 min using a flow rate of 1 ml min^{-1}. Sample preparation involved mixing 100 μl gel with acetronitrile/water (900 μl, 50:50 mixture) containing 0.1% trifluoroacetic acid. The samples were then filtered through a 0.45-μm syringe filter before injection. Further analysis by liquid chromatography-mass spectrometry (LC-MS) was carried out to verify the reaction products.

Circular dichroism. Spectra were measured on a Jasco J-810 spectropolarimeter with 1 s integrations with a step size of 1 nm and a single acquisition with a slit width of 1 nm due to the dynamic nature of the system. Time course experiments were conducted at 307 nm with data acquired every second with a 1-nm slit width. Materials

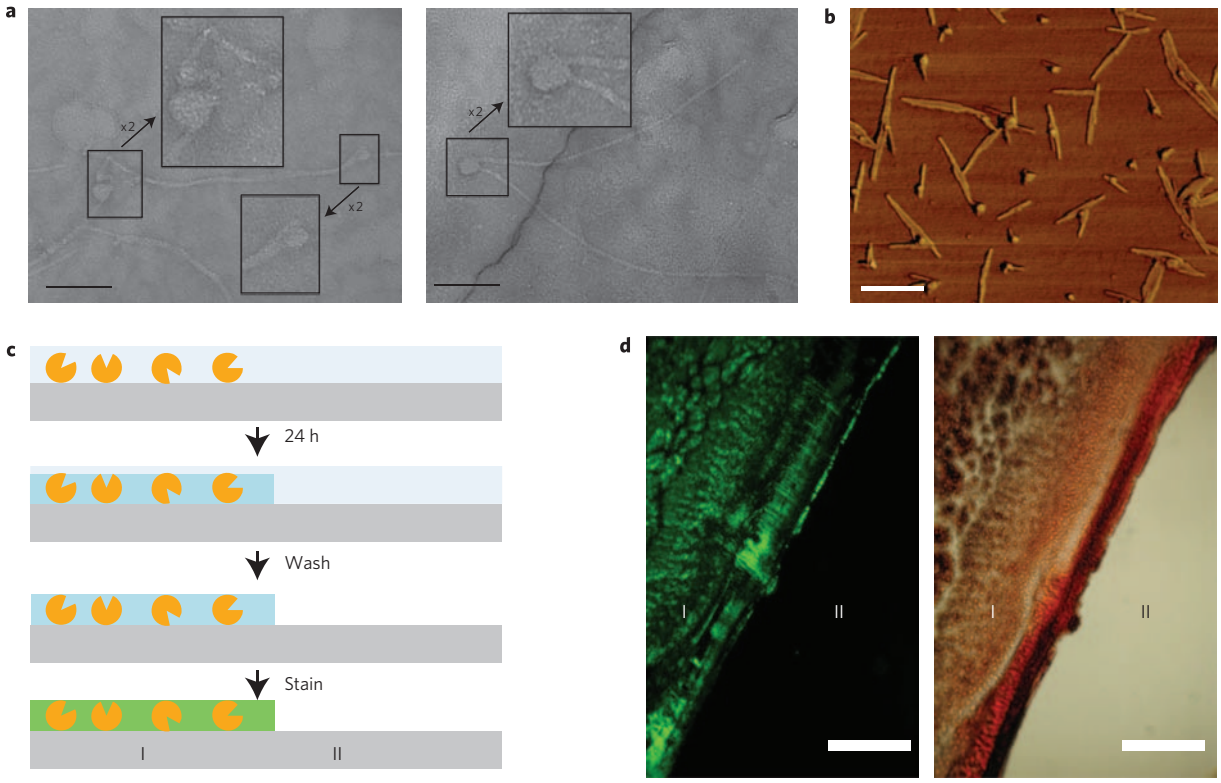

Figure 4 | Spatial confinement of nucleation and growth. a, TEM images of typical features observed with fibre propagation, demonstrating confined fibre growth from spherical structures (scale bars, 100 nm). **b**, The same process as visualized by AFM phase imaging (scale bar, 250 nm). **c**, Schematic of self-assembly using immobilized enzyme. The enzyme is coupled to the glass surface through PEG-diamine and glutaraldehyde crosslinking. When the reactant solution is introduced, self-assembly is observed after 24 h, exclusively in the area where immobilized enzyme is present. **d**, Localized self-assembly visualized by staining with Congo Red under cross-polarized light for an Fmoc-L/L_2 sample. The association of the dye with the β-sheet of the fibres results in green birefringence. No effect is observed on the regions without enzyme (scale bars, 0.3 mm).

were prepared as described above. The thermolysin was added at a concentration of 0.2 mg ml^{-1} and the resultant solution was analysed in a 0.5 mm quartz cell at 20 °C.

Infrared spectroscopy. Spectra were recorded on a Thermo Nicolet 5700 spectrometer with a smart ark plug-in attenuated total reflectance (ATR) unit with a zinc selenide trough plate. The samples were spread directly on the surface of the trough plate. Spectra were acquired in the 4,000 to 400 cm^{-1} range with a resolution of 4 cm^{-1} over 128 scans.

Transmission electron microscopy. Carbon-coated copper grids (No. 400) were glow discharged for 5 s and placed shiny side down on the surface of a 10 μl droplet containing 5 mM l^{-1} droplet of $_{dd}H_2O$ for 60 s and blotted. Washed grids were then place on a 10 μl droplet of freshly prepared and filtered 4% (w/v) uranyl acetate for 60 s and then blotted against double-folded Whatman 50 filter paper. Data were recorded in a Tecnai 10 TEM operating at 100 keV (calibrated magnification of ×43,600) onto Kodak SO-163 film. Images were subsequently scanned using a UMAX2000 transmission scanner providing a specimen level increment of 3.66 Å per pixel.

Atomic force microscopy. Trimmed mica sheets (Agar Scientific, UK) were adhered to AFM support stubs (Agar Scientific, UK) using clear nail varnish. Cleaved mica surfaces were prepared by removing the top layer of mica with adhesive tape immediately before sample deposition. The reactant solutions were mixed with enzyme and deposited slightly offset to the centre of the freshly cleaved mica surface and allowed to air dry overnight. Samples were imaged by intermittent contact mode in air using a Veeco Multimode atomic force microscope with a Nanoscope IIIa controller and an 'E' scanner. Imaging was performed using Olympus high-aspect-ratio etched silicon probes with nominal spring constant of 42 N m^{-1} (Veeco Instruments S.A.S.). Cantilever oscillation varied between 300 and 350 kHz while the drive amplitude was determined by the Nanoscope software. The setpoint was adjusted to just below the point at which tip–sample interaction was lost. Height and phase images with scan sizes of either 5 or 2 μm^2 were captured at a scan rate of 1.49 Hz and at a relative humidity of <40%. Data were first-order flattened using the Nanoscope software before image export. The instrument was periodically calibrated using a grating with 180-nm-deep, 10-μm^2 depressions.

Enzyme immobilization on a glass surface. Glass cover slips were immersed with 3 M NaOH for 5 min followed by a freshly prepared piranha solution (a typical mixture of 75% concentrated sulphuric acid and 25% of a 30% hydrogen peroxide solution, strongly corrosive) for 1 h. After rinsing with water, these glass cover slips were dried at 110 °C in an oven overnight. These glass slips were incubated with glycidyloxipropyltrimethoxysilane (GOPTS) at a surface concentration of ~5 μl cm^{-2} for 1 h, avoiding exposure to the atmosphere by assembling two cover slips face-to-face. Glass cover slips were then washed with dry acetone and dried in a nitrogen stream. Immediately, the surfaces were heated with the pure *O,O′-bis*(2-aminoethyl)octadecaethylene glycol (PEG-diamine) derivatives to melt them on the surface at 75 °C for 36 h. The surface was then thoroughly rinsed with water and dried at room temperature under a nitrogen stream. Glass cover slips were treated with a 2% solution of glutaraldehyde in 0.02 M Kpi buffer for 1 h at room temperature and thoroughly rinsed with buffer. A solution of enzyme (thermolysin or chymotrypsin, 5 mg in 1 ml 0.02 M Kpi buffer) was deposited to (partially) cover the surface, and the immobilization proceeded for 24 h at room temperature. The enzyme-modified surfaces were rinsed with 0.02 M Kpi buffer followed by water.

Congo Red staining and birefringence. A 50 μl solution of 20 mmol of Fmoc amino acids and amino acid methyl ester/peptide solution were incubated for 24 h in the presence of enzyme-modified surfaces in a screw cap glass vial, and allowed to dry on a glass microscope slide. Staining was performed by the addition of a 20 μl solution of 10 μM Congo Red in 100 mmol NaCl solution. Excess stained Congo Red was removed by rinsing with water several times and the slide was then dried. Birefringence was determined with a Zeiss Imager A1 microscope equipped with cross polarizers.

Fluorescence spectroscopy. Fluorescence emission spectra were measured on a Jasco FP-6500 spectrofluorometer with light measured orthogonally to the excitation light, with excitation at 295 nm and emission data range between 300 and 600 nm.

Received 11 September 2008; accepted 26 November 2008; published online 21 December 2008

References

1. Whitesides, G. M. & Boncheva, M. Beyond molecules: Self-assembly of mesoscopic and macroscopic components. *Proc. Natl Acad. Sci. USA* **99,** 4769–4774 (2002).
2. Lehn, J.-M. *Supramolecular Chemistry: Concepts and Perspectives* (VCH, 1995).
3. Jonkheijm, P., van der Schoot, P., Schenning, A. P. H. J. & Meijer, E. W. Probing the solvent-assisted nucleation pathway in chemical self-assembly. *Science* **313,** 80–83 (2006).
4. Silva, G. A. *et al.* Selective differentiation of neural progenitor cells by high-epitope density nanofibers. *Science* **303,** 1352–1355 (2004).
5. Zhang, S. G., Holmes, T., Lockshin, C. & Rich, A. Spontaneous assembly of a self complementary oligopeptide to form a stable macroscopic membrane. *Proc. Natl Acad. Sci. USA* **90,** 3334–3338 (1993).
6. Reches, M. & Gazit, E. Casting metal nanowires within discrete self-assembled peptide nanotubes. *Science* **300,** 625–627 (2003).
7. Kiyonaka, S. *et al.* Semi-wet peptide/protein array using supramolecular hydrogel. *Nature Mater.* **3,** 58–64 (2004).
8. Schenning, A. P. H. J. & Meijer, E. W. Supramolecular electronics; nanowires from self-assembled π-conjugated systems. *Chem. Commun.* **26,** 3245–3258 (2005).
9. Yang, Z. M. *et al.* Enzymatic formation of supramolecular hydrogels. *Adv. Mater.* **16,** 1440–1444 (2004).
10. Smith, A. M. *et al.* Fmoc-Diphenylalanine self assembles to a hydrogel via a novel architecture based on π–π interlocked β-sheets. *Adv. Mater.* **20,** 37–41 (2008).
11. Corbett, P. T. *et al.* Dynamic combinatorial chemistry. *Chem. Rev.* **106,** 3652–3711 (2006).
12. Rowan, S. J., Cantrill, S. J., Cousins, G. R. L., Sanders, J. K. M. & Stoddart, J. F. Dynamic covalent chemistry. *Angew. Chem. Int. Ed.* **41,** 898–952 (2002).
13. Sreenivasachary, N. & Lehn, J. M. Gelation-driven component selection in the generation of constitutional dynamic hydrogels based on guanine-quartet formation. *Proc. Natl Acad. Sci. USA* **102,** 5938–5943 (2005).
14. Winkler, S., Wilson, D. & Kaplan, D. L. Controlling β-sheet assembly in genetically engineered silk by enzymatic phosphorylation/dephosphorylation. *Biochemistry* **39,** 12739–12746 (2000).
15. Yang, Z., Liang, G., Ma, M., Gao, Y. & Xu, B. *In vitro* and *in vivo* enzymatic formation of supramolecular hydrogels based on self-assembled nanofibers of a β-amino acid derivative. *Small* **3,** 558–562 (2007).
16. Dos Santos, S. *et al.* Switch-peptides: Controlling self-assembly of amyloid β-derived peptides *in vitro* by consecutive triggering of acyl migrations. *J. Am. Chem. Soc.* **127,** 11888–11889 (2005).
17. Hu, B.-H. & Messersmith P. B. Rational design of transglutaminase substrate peptides for rapid enzymatic formation of hydrogels. *J. Am. Chem. Soc.* **125,** 14298–14299 (2003).
18. Um, S. H. *et al.* Enzyme-catalysed assembly of DNA hydrogel. *Nature Mater.* **5,** 797–801 (2006).
19. Carpenter, F. H. The free energy change in hydrolytic reactions. The non-ionized compound convention. *J. Am. Chem. Soc.* **82,** 1111–1122 (1960).
20. Toledano, S., Williams, R. J., Jayawarna, V. & Ulijn, R. V. Enzyme-triggered self-assembly of peptide hydrogels via reversed hydrolysis. *J. Am. Chem. Soc.* **128,** 1070–1071 (2006).
21. Oh, K., Jeong, K.-S. & Moore, J. S. Folding-driven synthesis of oligomers. *Nature* **414,** 889–893 (2001).
22. Bilgicer, B., Xing, X. & Kumar, K. Programmed self-sorting of coiled coils with leucine and hexafluoroleucine cores. *J. Am. Chem. Soc.* **123,** 11815–11816 (2001).
23. Krishnan-Ghosh, Y. & Balasubramanian, S. Dynamic covalent chemistry on self-templating peptides: Formation of a disulfide-linked β-hairpin mimic. *Angew. Chem. Int. Ed.* **42,** 2171–2173 (2003).
24. Case, M. A. & McLendon, G. L. A virtual library approach to investigate protein folding and internal packing. *J. Am. Chem. Soc.* **122,** 8089–8090 (2000).
25. Swann, P. G. *et al.* Nonspecific protease-catalyzed hydrolysis synthesis of a mixture of peptides: Product diversity and ligand amplification by a molecular trap. *Biopolymers* **40,** 617–625 (1996).
26. Forster, T. Excimers. *Angew. Chem. Int. Ed.* **8,** 333–343 (1969).
27. Pinion, J. P., Minn, F. L. & Filipescu, N. Excimer emission from dibenzofuran and substituted fluorenes. *J. Lumin.* **3,** 245–252 (1971).
28. Aggelli, A. *et al.* Responsive gels formed by the spontaneous self-assembly of peptides into polymeric β-sheet tapes. *Nature* **386,** 259–262 (1997).
29. Lins, R. J., Flitsch, S. L., Turner, N. J., Irving, E. & Brown, S. A. Enzymatic generation and *in situ* screening of a dynamic combinatorial library of sialic acid analogues. *Angew. Chem. Int. Ed.* **41,** 3405–3407 (2002).
30. Mann, S. Life as a nanoscale phenomenon. *Angew. Chem. Int. Ed.* **47,** 5306–5320 (2008).

Acknowledgements

We thank the Engineering and Physical Sciences Research Council and the Leverhulme Trust for funding, P. Crook for assistance with infrared spectroscopy, S. Todd for assistance with surface modification, P. Coppo and T. Jowitt for assistance with fluorescence, and V. Barittini for mass spectrometry. N.H. acknowledges the support of the UK Centre for Tissue Regeneration (a partnership between NorthWest Development Agency and University of Manchester, UK). R.V.U. acknowledges P. Halling for his careful reading of the manuscript and for providing helpful suggestions.

Author contributions

R.V.U. conceived the concepts and helped design the experiments. R.J.W., A.K.D., A.M.S., R.C. and N.H. designed and performed the experiments and analysed the data. All authors co-wrote the paper.

Additional information

Supplementary Information accompanies this paper at www.nature.com/naturenanotechnology. Reprints and permission information is available online at http://npg.nature.com/reprintsandpermissions/. Correspondence and requests for materials should be addressed to R.V.U.